ELECTRIC CURRENTS DISTRIBUTIONS ON FINITE PATCH CONDUCTOR OF MICROSTRIP ANTENNA

Takafumi FUJIMOTO, Kazumasa TANAKA, Mitsuo TAGUCHI
Dept. of Electrical & Electronic Eng., Nagasaki University
1-14 Bunkyo-machi, Nagasaki-shi, 852-8521, Japan
E-mail: takafumi@net.nagasaki-u.ac.jp

The electric currents on the upper, lower and side surfaces of the finite patch conductor of a circular microstrip antenna are calculated by using the method of moment in the spectral domain. The electric current on the lower surface is much bigger than that on the upper surface and the input impedance of microstrip antenna depends on the electric current on the lower surface.

1. Introduction

The thickness of the patch conductor of microstrip antenna (MSA) is finite. Therefore, the electric currents exist on the upper, lower and side surfaces of the patch conductor. However, in the analysis of MSA by the method of moment in the spectral domain (SD-MoM)[1, 2], the patch conductor is assumed to be infinitely thin and the total current on the upper and lower surfaces of the patch conductor is derived.

Authors have derived the electric currents on the upper and lower surfaces of the patch conductor of a circular MSA separately by using SD-MoM [3]. In reference [3], since the current on the side surface has been neglected, the continuity of the currents on the upper, lower and side surfaces of the patch conductor hasn't been considered.

In this paper, the electric currents on the upper, lower and side surfaces of the patch conductor of a circular MSA are derived by using SD-MoM. The integral equations are derived from the boundary condition that the tangential component of the total electric field due to the electric currents on the upper, lower and side surfaces of the patch conductor vanishes on the upper, lower and side surfaces of the patch conductor. The electric fields on the upper, lower and side surfaces of the patch conductor are derived by using Green's functions in the spectral domain produced by the vertical and horizontal electric dipoles on those surfaces.

In order to investigate the effects of the currents on upper, lower and side surfaces to the antenna characteristics, the input impedances due to those currents are calculated.

2. Theory

Fig. 1 shows the geometry of a circular MSA and its coordinate system. The radius and thickness of the circular patch conductor are a_0 and δ_z, respectively. The relative dielectric constant and thickness of the dielectric substrate are ε_r and h, respectively. The antenna is excited at $r = d_0$, $\phi = 0^\circ$ by a coaxial feeder through the dielectric substrate.

Fig. 2 shows an analytical model of the circular MSA. The electric currents on the upper, lower and side surfaces of the patch conductor are denoted by $\mathbf{J}^U$, $\mathbf{J}^L$ and $\mathbf{J}^S$, respectively. The currents on the patch conductor follow closely the behavior of the corresponding eigenmode within the cavity bounded above and below by the conducting plates and on the side by the admittance wall [4]. Therefore, $\mathbf{J}^U$, $\mathbf{J}^L$ and $\mathbf{J}^S$ are expressed as

$$\mathbf{J}^p = \sum_{m=0}^{M}\sum_{n=0}^{N} A^p_{mn} F^p_{rmn}(r,\phi)\mathbf{i}_r + \sum_{m=0}^{M}\sum_{n=1}^{N} B^p_{mn} F^p_{\phi mn}(r,\phi)\mathbf{i}_\phi \tag{1a}$$

$$F^p_{rmn} = U_m\left(\frac{r}{a_0}\right)\left\{1-\left(\frac{r}{a_0}\right)^2\right\}^{\nu^p}\cos(n\phi), \quad m+n = \text{even} \tag{1b}$$

$$F^p_{\phi mn} = T_m\left(\frac{r}{a_0}\right)\left\{1-\left(\frac{r}{a_0}\right)^2\right\}^{\nu^p-1}\sin(n\phi), \quad m+n=\text{odd}, \tag{1c}$$

$$\mathbf{J}^S = \sum_{m=0}^{M}\sum_{n=0}^{N} A^S_{mn}F^S_{zmn}(\phi,z)\mathbf{i}_z + \sum_{m=0}^{M}\sum_{n=1}^{N} B^S_{mn}F^S_{\phi mn}(\phi,z)\mathbf{i}_\phi \tag{2a}$$

$$F^S_{zmn} = U_m\left(\left|1-\frac{2z}{\delta_z}\right|\right)\left\{1-\left(1-\frac{2z}{\delta_z}\right)^2\right\}^{\nu^S} \times\cos(n\phi), \quad m+n=\text{even} \tag{2b}$$

$$F^S_{\phi mn} = T_m\left(\left|1-\frac{2z}{\delta_z}\right|\right)\left\{1-\left(1-\frac{2z}{\delta_z}\right)^2\right\}^{\nu^S-1} \times\sin(n\phi), \quad m+n=\text{odd}. \tag{2c}$$

Where, p is U or L and ν^S is equal to ν^U for $\delta_z/2 \leqq z \leqq \delta_z$ and ν^L for $0 \leqq z \leqq \delta_z/2$. T_n and U_n are Chebyshev polynomials of the first and second kind, respectively. $\{A^p_{mn}\}$ and $\{B^p_{mn}\}$ are unknown coefficients. Since the currents must be continuity at the center of the circular patch, the sums of m and n with respect to the r and ϕ components of the currents are even and odd, respectively. The edge conditions of the currents on the metallic 90° corner are used. Therefore, ν^U is 0.667 and ν^L is 0.603 for $\varepsilon_r = 2.15$ [5].

The electric fields on the upper, lower and side surfaces of the patch conductor produced by $\mathbf{J}^p(p = U, L, S)$ are denoted by $\mathbf{E}^U(\mathbf{J}^p)$, $\mathbf{E}^L(\mathbf{J}^p)$ and $\mathbf{E}^S(\mathbf{J}^p)$, respectively. The excitation fields due to the feed current $\mathbf{J}^e$ are denoted by $\mathbf{E}^U(\mathbf{J}^e)$, $\mathbf{E}^L(\mathbf{J}^e)$ and $\mathbf{E}^S(\mathbf{J}^e)$. The boundary conditions on the upper, lower and side surfaces of the patch conductor are expressed as

$$\left\{\sum_{p=U,L,S}\mathbf{E}^q(\mathbf{J}^p)+\mathbf{E}^q(\mathbf{J}^e)\right\}\times\mathbf{n}=\mathbf{0} \quad \text{on } S_q,\ q=U,L,S, \tag{3}$$

where $\mathbf{n}$ is the unit normal vector directed outward from the patch conductor and S_U, S_L and S_S are the upper, lower and side surfaces of the patch conductor, respectively.

In the formulation of the electric fields, the local coordinate system (X, Y, Z) with the origin located at the point $(r', \phi', 0)$ is used. Fig. 3 shows the local coordinate system (X, Y, Z). The positive X direction is defined by the tangential ϕ' direction. $\mathbf{E}^q(\mathbf{J}^p)$ is expressed by the vector potential $\mathbf{A}^q(\mathbf{J}^p)$ and the scalar potential $\phi^q_e(\mathbf{J}^p)$;

$$\mathbf{E}^q(\mathbf{J}^p) = -j\omega\mathbf{A}^q(\mathbf{J}^p) - \nabla\phi^q_e(\mathbf{J}^p) \tag{4}$$

$$\mathbf{A}^q(\mathbf{J}^p) = \int_{S_p}\Big\{(\mathbf{i}_X G^{XX}_A + \mathbf{i}_Z G^{ZX}_A)\mathbf{i}_X + (\mathbf{i}_Y G^{YY}_A + \mathbf{i}_Z G^{ZY}_A)\mathbf{i}_Y + (\mathbf{i}_X G^{XZ}_A + \mathbf{i}_Y G^{YZ}_A + \mathbf{i}_Z G^{ZZ}_A)\mathbf{i}_Z\Big\}\cdot\mathbf{J}^p dS' \tag{5}$$

$$\phi^q_e(\mathbf{J}^p) = -\frac{1}{j\omega}\int_{S_p} G_U(\nabla'\cdot\mathbf{J}^p)dS'. \tag{6}$$

Where G^{ST}_A is S component of Green's function for the vector potential due to a T- directed electric dipole and G_U is Green's function for the scalar potential. ∇ and ∇' are the derivative operators at the observation and source points. $\mathbf{i}_X$, $\mathbf{i}_Y$ and $\mathbf{i}_Z$ are unit vectors of the local coordinate system (X, Y, Z). By substituting eqns. (4)–(6) into eqn. (3), the integral equations are obtained. $\{A^p_{mn}\}$ and $\{B^p_{mn}\}$ are determined by applying the method of moment to the integral equations.

Green's functions in the spectral domain are obtained by applying the solutions of the wave equations in the spectral domain to the boundary conditions at the interfaces between the air, the dielectric and the ground plane and the radiation condition. Green's functions in the spatial domain are derived by applying the inverse Fourier transform to Green's functions in the spectral domain [1][6].

3. Results and Discussion

Figs. 4(a)–(d) show the calculated $\mathbf{J}^U$, $\mathbf{J}^L$ and $\mathbf{J}^S$ at the resonant frequency (6.33GHz). The intensity of $\mathbf{J}^L$ is bigger than that of $\mathbf{J}^U$ and the phase of $\mathbf{J}^L$ is nearly equal to that of $\mathbf{J}^U$. Although the intensity of J^S_z is very small compared with those of J^U_r and J^L_r, the intensity of J^S_ϕ is much bigger than those of J^U_ϕ and J^L_ϕ.

Figs. 5(a) and (b) show the calculated input impedances. $\mathbf{J}^U$ and $\mathbf{J}^S$ don't contribute to the input impedance. This is due to facts that the intensity of $\mathbf{J}^U$ is small compared with that of $\mathbf{J}^L$ and the thickness of the patch conductor δ_z is very small compared with the radius of the circular patch conductor a_0.

4. Conclusion

The electric currents on the upper, lower and side surfaces of the finite patch conductor have been calculated by SD-MoM. The integral equations are derived from the boundary condition on the upper, lower and side surfaces of the patch conductor. The electric fields on upper, lower and side surfaces of the patch conductor are derived by using Green's functions in the spectral domain produced by the vertical and horizontal electric dipoles on those surfaces. The electric current on the lower surface is much bigger than that on the upper surface. The input impedance of the MSA depends on the electric current on the lower surface.

References

[1] J.R. Mosig, "Integral equation technique, " ed. T. Itoh, in Numerical techniques for microwave and millimeter-wave passive structures, pp.133–213, John Wiley & Sons, New York, 1989.

[2] K. Araki and T. Itoh, "Hankel transform domain analysis of open circular microstrip radiating structures, " IEEE Trans., Antennas Propagat., Vol. AP-29, No. 1, pp.84–89, Jan. 1981.

[3] T. Fujimoto, K. Tanaka and M. Taguchi, "Comparison of currents on upper and lower sides of patch conductor of microstrip antenna," Proc. IEEE AP-S. Int. Symp., Vol. 4, pp.170–173, June 2002.

[4] T. Fujimoto, K. Tanaka and M. Taguchi, "Wall admittance of a circular microstrip antenna," IEICE Trans. Commun., Vol. E82-B, No. 5, pp.760–767, May 1999.

[5] J. V. Bladel, "Field singularities at metal-dielectric wedges, " IEEE Trans., Antennas Propagat., Vol. AP-33, No. 4, pp.450–455, April 1985.

[6] K. A. Michalski and D. Zheng, "Electromagnetic scattering and radiation by surfaces of arbitrary shape in layered media, Part I : Theory, " IEEE Trans., Antennas Propagat., Vol. AP-38, No. 3, pp.335–344, March 1990.

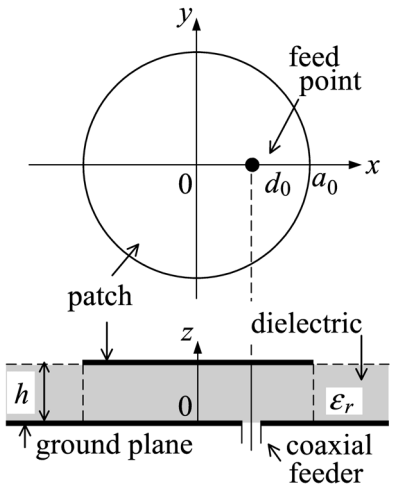

Fig. 1 Circular MSA

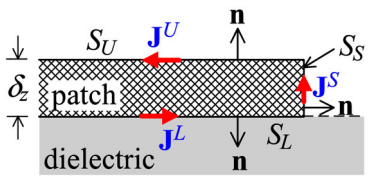

Fig. 2 Analytical model (cross section)

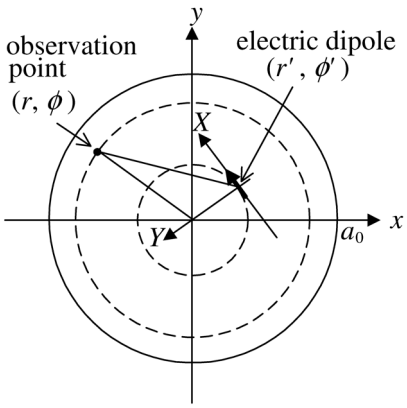

Fig. 3 Local coordinate system

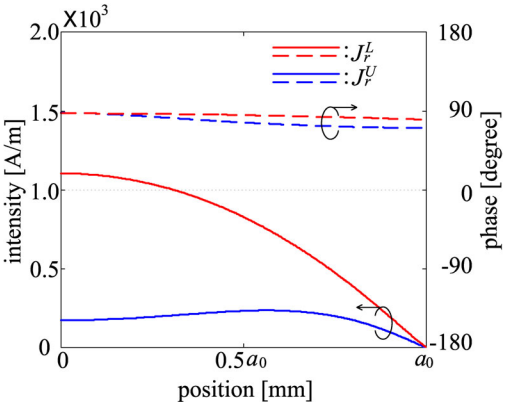

(a) J_r^U, J_r^L $(\phi = 0°)$

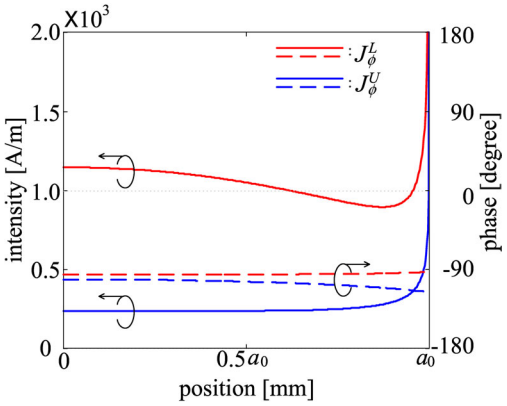

(b) J_ϕ^U, J_ϕ^L $(\phi = 90°)$

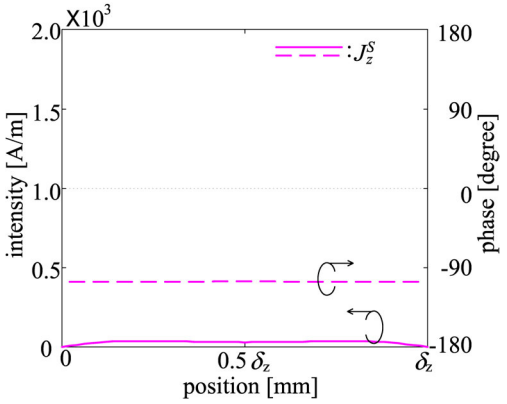

(c) J_z^S $(\phi = 0°)$

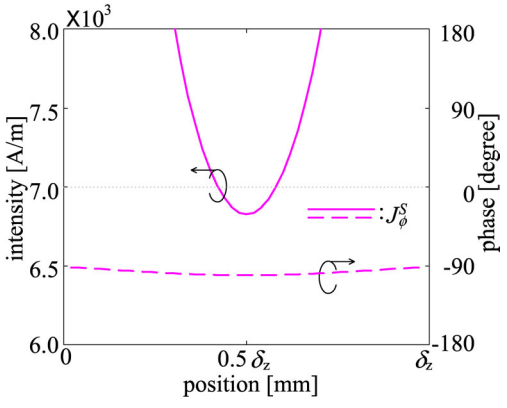

(d) $J_\phi^S(\phi = 90°)$

Fig. 4 Electric currents distributions

(a_0=9.06mm, d_0=6.0mm, h=0.764mm, ε_r=2.15, δ_z=0.018mm, M=N=3, frequency=6.33GHz)

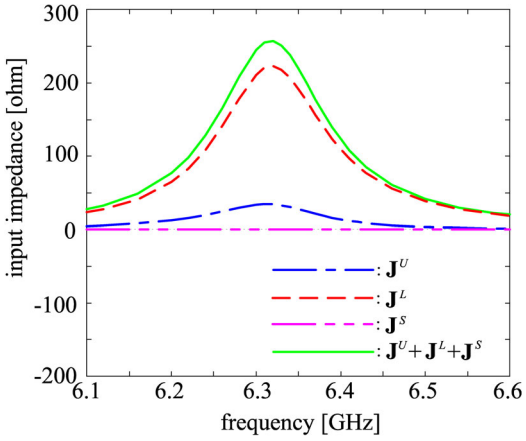

(a) Input resistances

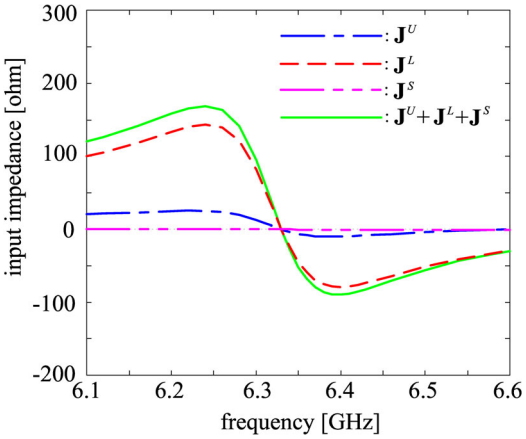

(b) Input reactances

Fig. 5 Input impedances

(a_0=9.06mm, d_0=6.0mm, h=0.764mm, ε_r=2.15, δ_z=0.018mm, M=N=3)